NASA CR 151,945

# FINAL REPORT ON THE INVESTIGATION OF HYDROGEN AND HELIUM PUMPING BY SPUTTER ION PUMPS FOR JUPITER AND OUTER PLANETS MASS SPECTROMETER

By Burton W. Scott, PhD

January 1977



(NASA-CR-151945) INVESTIGATION OF HYDROGEN AND HELIUM PUMPING BY SPUTTER ION PUMPS FOR JUPITER AND OUTER PLANETS MASS SPECTROMETER (Perkin-Elmer Corp.) 44 p HC A03/MF A01 CSCL 03E G3/91

N77-17985

Unclas 14989

Prepared under Contract No. NAS2-9116 by
Perkin-Elmer Corporation
Aerospace Division
Pomona, California

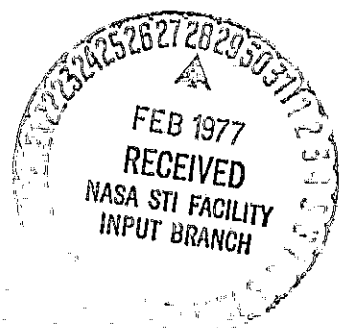


for

AMES RESEARCH CENTER

NATIONAL AERONAUTICS AND SPACE ADMINISTRATION

Moffett Field, California 94035

TABLE OF CONTENTS



LIST OF ILLUSTRATIONS

LIST OF ILLUSTRATIONS (Concluded)

# INVESTIGATION OF HYDROGEN AND HELIUM PUMPING BY SPUTTER ION PUMPS FOR THE JUPITER AND OUTER PLANETS MASS SPECTROMETER

## 1. INTRODUCTION

The purpose of this study is to investigate the suitability of a small ion pump for maintaining the vacuum of a mass spectrometer analyzer used as a Jupiter Atmosphere probe.

The most abundant gases on Jupiter are hydrogen and helium. The column abundance of hydrogen has been deduced from ground-based spectroscopic observations, and helium has been detected by ultraviolet photometry on board Pioneers 10 and 11. The helium/hydrogen ratio is expected to be about 10%, but present knowledge is imprecise, so a measure of this would be very important on the Jupiter probe. The next most prevalent species comprises less than $10^{-3}$ of the atmosphere. Below this level, there are many trace constituents which are likely to be present at concentrations which are orders of magnitude lower. The instrument requirements as established by Kennedy[1], et al, therefore, include a measure of the helium/hydrogen ratio to 1% accuracy and trace constituent measurements with a dynamic range of $1:10^6$ over the mass range 2-52 AMU. With sample enrichment in hydrogen and helium by a factor of $10^2$, at least some of the minor constituents in the atmosphere may be measured in the low ppb ($1:10^9$) range[2]. The gases are measured as the probe descends through the atmosphere during a time period of less than 30 minutes. Samples are taken at altitudes corresponding to $10^4$ Pa (0.1 bar) and $10^6$ Pa (10 bars), with the first decade being traversed in approximately two minutes.

The mission requirement can only be realized by the mass spectrometer analyzer if the partial pressures in the ion source can be related in a known way to the partial pressures in the atmosphere. Mixing ratios are more important than absolute values. Aside from the helium/hydrogen ratio goal of 1% accuracy, other accuracy goals depend on the ratio in question. In many cases a ratio accuracy of 2-5% is required for useful information, and in other cases an order of magnitude determination might prove very interesting. To achieve these accuracies we must limit all sources of sample modification. Sample modification can, of course, occur anywhere in the stream from the atmosphere through the sampling lines into the mass spectrometer leak, in the ion source and on into the pump. The pump performance can be a strong influence once the sample is past the inlet leak.

Choosing the inlet line, leak, ion source, and pump involves various trade-offs that may vary from one instrument to another, but certain guidelines have become established. First, since the source should contain only gas entering through the leak, it is designed to have low conductance to the analyzer-pump region. Other design considerations fix the total conductance of a single electron beam aperture and ion beam object slit at about 40 cc/s for nitrogen. A useful sample pressure in the source is about $10^{-4}$ torr, high enough to give good sensitivity, yet still safely below the region where ion space charge effects may modify the output signals. The sample flow is thus established at around $4 \times 10^{-3}$ torr cc/s referenced to nitrogen. The source sample can be modified by flow of residual gas from the analyzer-pump region back into the source. To minimize this effect, the analyzer pressure should be kept as low as possible by employing a large capacity pump. A useful parameter in describing this effect is the differential pumping factor found by the ratio of the pump speed to the source conductance.

Previous mass spectrometer analyzers have been found to reliably measure partial pressures of common gas mixes to a precision of 1% when the differential pumping factor was 100, implying a pump speed of four liter/second used with the 40 cc per second source. These speeds and conductances refer strictly to nitrogen but hold generally for air and many other gases. Since the molecular conductance of the source and pump are inversely proportional to the square root of the sample molecular weight, a 40 cc/s nitrogen conductance becomes 106 cc/s for helium and 150 cc/s for hydrogen. Further, a review of manufacturers specifications and literature reveals that most ion pumps pump helium at a speed less than 30% of that of nitrogen. Therefore, specifying a pump which would maintain a differential pumping factor of 100 for helium, implies a pump with a nitrogen speed of 30 ℓ/s. A pump with this capacity would weigh in excess of 12 kg as well as occupy an excessive volume for an interplanetary mission. For this reason, it is appropriate to review the ion pumping of hydrogen and helium, quantify the effect a practical pump would have on sample modification, and explore alternatives to the brute force method of employing a large pump.

The pumping of hydrogen and helium with emphasis on short duration runs is an area that has received relatively little attention in most ion pump studies and theories. The emphasis is normally on steady state performance, and the transient behaviour of the pump is carefully ignored. In addition, most theories consider helium and argon together as far as pumping mechanisms go. Indeed, argon has received a great deal of attention in both theory and design of the pump, but it is not obvious that helium performance is optimized in the same way as argon performance.

The study presented here, therefore, reviews the phenomena of ion pumping with emphasis on the pumping mechanism for hydrogen and helium. The experimental tests measure the performance of a small, flight proven ion pump which has a nominal four liter/second pumping speed for air. The speed of this pump for hydrogen and helium, and for hydrogen/helium mixes is presented with particular detail regarding the time dependence.

The results of the pump tests are then related to anticipated performance of the mass spectrometer by relating the pumping speeds for the gases to the partial pressure in the ion source. From this analysis, the pump specifications are quantified in terms of mission goals and in terms of observed pumping speeds for helium, hydrogen, helium/hydrogen mixes, various load levels, and time periods.

In addition to pumping speeds with helium and hydrogen, the phenomenon of pump memory will have important consequences on the mass spectrometer performance. This is the phenomenon of gases being generated in the pump when a load of sample gas is introduced. These gases can be either previously pumped gases which evolve from the pump, or they can be species formed in the pump. Also, some gases come out of the pump even with no gas load. These background gases lead to a background spectrum which can be subtracted. The pump memory gases will have the same partial pressures in the source as in the analyzer, so it is important to examine the extent they will limit measurements of the minor constituents in the Jovian atmosphere. Therefore, the second part of the experiments presented here is concerned with a measure of partial pressures of every residual gas over the mass range 2-52, both with and without sample gas loads. These memory gases are then compared with the anticipated mixing ratios in the Jovian atmosphere and their effect on the measurements is discussed.

# 2. ION PUMP THEORY

## 2.1 THE GEOMETRY AND THE ELECTRON CLOUD DENSITY

A cross sectional view of a single cell ion pump is shown in Figure 2-1. It consists of a cylindrical anode located between a pair of cathode plates. When voltage and magnetic field are applied, a cold cathode Penning discharge can be maintained over a wide range of pressures. Electrons in the discharge are constrained by the magnetic field from proceeding directly to the anode. Electrons emitted from the cathodes (by positive ion bombardment, for example) proceed to the anode by a series of ionizing collisions with gas molecules. The electrons produced from these collisions are also trapped in the magnetic field, thus adding to the discharge. The overall geometry of the cell diameter, d, length, and spacing is dictated by this requirement of trapping the electrons. The cell diameter, in other words, must be large compared to the electron orbit diameters for the voltage and magnetic field, B, used. Since electron orbit diameter is inversely proportional to magnetic field, this implies constant Bd product.

The number of electrons multiplies in the discharge until it significantly alters the electric fields in the cathode-anode space. This charge density then alters the trajectories of newly formed electrons from the cathode and elsewhere, so that they cannot enter the discharge. The discharge is thus space charge limited.

The density of the space charge is constant over several decades of pressure below $10^{-4}$ torr, since the electron density is orders of magnitude higher than the ion density. Thus the number of ions formed is proportional to the neutral gas density. This means that the pumping speed is constant, independent of pressure, providing that the ions formed have no effect on the processes by which they are pumped.

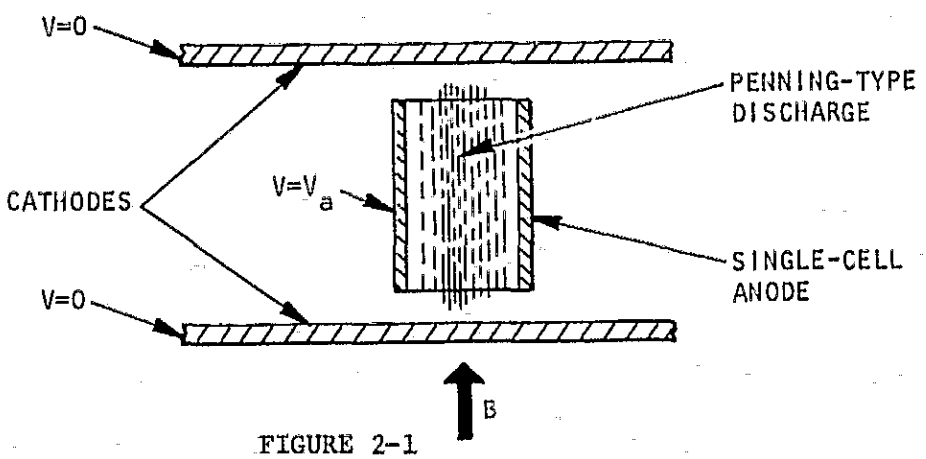


FIGURE 2-1

Cross-Sectional Side View of a Single-Cell Vacion Pump

These conditions have been verified experimentally over gas loads, pressures and geometries that have been found useful for a mass spectrometer analyzer pump. Exceptions are encountered at high and low pressures, usually meaning that the pumping speed drops off. These conditions, however, are of only minimal interest in this study and so will be ignored.

The amount of space charge that can be trapped in the cylindrical anode structure can be shown to be limited to:[3]

$$Q = 1.11 \times 10^{-12} \text{ VL coulombs}$$

where V is the space charge depression, and L is the cell length

This follows from the divergence equation of the electric field in cylindrical coordinates. This value is independent of anode diameter, which is governed by the previous relation concerning the electron orbit radii. Since the trapped charge is independent of anode diameter, increased pumping speed (more electron charge) is obtained by increasing the number of cells instead of simply increasing their size. This possibility is discussed more fully later in this section.

Since the electron cloud density is constant, independent of pressure, the discharge current, I, will depend only on the rate of ionization of the neutral molecules. The current is thus proportional to pressure, P. The constant of proportionality is the discharge intensity; $I_p$

$$I_p = I/P \quad \text{amps-torr}^{-1}$$

A rough estimate for the discharge intensity can be derived from known cross sections for ionization by electron impact. Since the current is given by the rate of formation, $\tau_c$, of ions:

$$I = \frac{-Q}{\tau_c}$$

$\tau_c$ is also the average collision rate for electrons in the cloud. The mean free path, $\lambda$, between collisions is:

$$\lambda = \frac{1}{\sigma \cdot N} \quad \text{cm}$$

where $\sigma$ = ionization cross section, $\text{cm}^2$

$N = 3.5 \times 10^{16}$ molecules $\text{cm}^{-3}$ - $\text{torr}^{-1}$

$$\tau_c = \frac{\lambda}{v}$$

where $v$ = electron velocity.

Assuming 100 eV electrons and $3 \times 10^{-16}$ $cm^2$ ionization cross section, we find

$$\tau_c P = 1.6 \times 10^{-10} \text{ torr/s}$$

The discharge intensity for each anode cell is then

$$\frac{I}{P} = \frac{-Q}{\tau_c P} = 6.94 \times 10^{-3} \text{ VL amp/torr}$$

Assuming a typical geometry, voltage and magnetic field, the discharge intensity is about 55 amp/torr for a 1/2 inch diameter, 0.8 inch long cell with 3.5 kV applied and a magnetic field of 1100 gauss.

This is an unrealistically high figure, since a more detailed analysis would find a distribution of charge that includes end effects and does not depress the potential completely to the cathode potential. In addition, the electrons will have a spread in energies, thus modifying the velocity, mean free path, and cross-section terms. In view of these approximations, the agreement, however, is good, and the derivation serves to illustrate how the discharge intensity depends on voltage, cell geometry, and ionization cross section.

The discharge intensity can be related to an ideal pumping speed, S, which assumes all ions are pumped. Since there are $3.5 \times 10^{19}$ molecules per torr/liter, and $6.2 \times 10^{18}$ ions per coulomb:

$$S = \frac{6.2 \times 10^{18}}{3.5 \times 10^{19}} \cdot \frac{I}{P} = 0.18 \frac{I}{P} \text{ liter-s}^{-1}\text{-cell}^{-1}$$

From these relations, it is possible to look for methods of increasing the discharge intensity within a given pump envelope size, i.e., by increasing voltage, cell length, or number of cells. Cell length, magnetic field, and voltage, of course, require trade-offs in the overall pump, pump magnet, and power supply combination. Without going into these in detail we can assume that existing flight designs represent some kind of optimized trade-off of these parameters and that there is not a great deal to be gained by further modifications. The choice of optimum cell diameter is more subtle.

The cell diameter has been found by Rutherford[4] to be an important parameter which controls a low-pressure mode change, where the discharge intensity falls off and pumping speed drops. This is apparently related to total path length of the electrons, and their inability to form a Townsend avalanche at the lower pressures. Electrons then leave the cloud, reach the anode, and decrease the probability of ionization. It is not clear from Rutherford's work how to quantify this effect, and he does not experimentally investigate any diameters less than 1/2 inch. It does appear, however, that the pumping speed at $10^{-6}$ torr can be increased by using more smaller cells in the same envelope. This change would result in lower speeds at lower pressures. Lower pressures are not important in the steady-state operation of the mass spectrometer, but there may be problems in starting the pump. This is an area which can be usefully investigated.

## 2.2 PUMPING PROCESSES

The foregoing discussion shows how the ions are formed in the discharge. Pumping does not occur until the ions penetrate the interior or are stably absorbed on the surfaces of the pump parts. Many phenomena are occurring simultaneously in the pump, and it is impossible to separate the various effects completely. The discussion presented here, is based on established thinking among ion pump researchers, with some modification based on recent sputtering investigations and ion scattering investigations.

The following processes are involved in the pumping of various gases by an ion pump. Starting with the space charge limited electron cloud in the Penning discharge, neutrals entering the cloud are ionized by electron impact and accelerated to the cathode. As they strike the cathode, they interact energetically with the conduction electrons and with the lattice atoms. This interaction can result in ejection of electrons, target atoms, previously pumped particles, or reflection of the incident particle either as an ion or neutral. If reflected as a neutral, it is then free to strike the anode or other surfaces and repeat the energetic processes. Pumping depends on the removal of ions or neutrals by burial in the cathode or anode, with or without chemical combination. Since gases differ in mass, ionization cross section, and chemical activity, they also differ in pumping speeds. A few sample calculations will show the relative importance of these processes for four gases: hydrogen, helium, nitrogen and argon. Hydrogen and helium are chosen because they are the subject of this report, nitrogen because it represents the dominant pumping process for most chemically active gases, and argon because it represents an informative comparison for helium. A pressure of $10^{-5}$ torr is considered in each case. The cathode material is assumed to be titanium.

The calculation of the various processes occurring in the pump follows from the electron cloud density calculated in Section 2.1, and from the ionization cross section and the sputtering rate. To start, we will assume that the various approximations leading to the charge in the electron cloud overestimates the ion production by a factor of 2. From there we can calculate the discharge intensity, I/P, the ion flux, and the cathode erosion rate for the four gases.

The ionization cross section in Table 2-1 is quite accurate. The sputter yield should be regarded as an estimate extrapolated from the related experimental data. The penetration depth is also an estimate based on several different types of experiments. Both the sputter yield and penetration depth are sufficiently accurate for an order of magnitude estimate of the surface processes occurring in the pump.

These sample calculations show the following important differences between these four gases in the ion pump: hydrogen has an ionization cross-section lower than nitrogen or argon and hence the rate of production of ions is low. Also, the sputter yield is low so the erosion due to hydrogen is insignificant. On the other hand, hydrogen ions can penetrate quite deeply. Note that the hydrogen penetrates to a mean depth that even argon would take several hours to erode away. In addition, there is very likely to be a high initial pumping

of hydrogen right from the gas phase by absorption on fresh surfaces followed by diffusion to the interior. Helium is notable because of its very low ionization cross-section, and consequently low discharge intensity. It likewise has negligible sputtering coefficient and deep penetration. In the cases of nitrogen and argon, we find a situation where the erosion rate is such that the mean penetration depth is uncovered after several minutes of operation. This situation is most critical in the case of argon where the maximum erosion rate is coupled with the lowest penetration.

TABLE 2-1

Ionization and Surface Processes Related to Sputter Ion Pumping

| | $H_2$ | He | $N_2$ | A |
|---|---|---|---|---|
| Ionization Cross Section[5] Maximum ($10^{-16}$ $cm^2$) | 0.95 | 0.35 | 2.70 | 3.25 |
| Sputter Yield 1 keV Ions[6] on Ti Target (atoms-$ion^{-1}$) | 0.01 | 0.05 | 0.2 | 0.4 |
| Discharge Intensity (amps-$torr^{-1}$) | 8.8 | 3.25 | 25 | 30 |
| Ion Flux at Cathode at $10^{-5}$ torr (ions-$cm^{-2}$-$s^{-1}$) | $2.68 \times 10^{13}$ | $0.99 \times 10^{13}$ | $7.61 \times 10^{13}$ | $9.4 \times 10^{13}$ |
| Erosion Rate (Atomic layer-$s^{-1}$) | $.016 \times 10^{-2}$ | $.03 \times 10^{-2}$ | $.92 \times 10^{-2}$ | $2.2 \times 10^{-2}$ |
| Penetration, mean range,[7] 1 keV ions on Ti target, (Atomic layers) | 200 | 100 | 20 | 10 |

Now we arrive at the pumping mechanism. From the above discussion, it is apparent that cathode burial is a possible mechanism for hydrogen and helium but not for argon and nitrogen. Nitrogen, and other active gases combine chemically with titanium and so the continual plating of the titanium on the other pump surfaces combining with the nitrogen is the most likely pumping process. The rate of sputtered titanium atoms could account for a pumping speed of 0.89 liters-$s^{-1}$-$cell^{-1}$ in our model if each sputtered atom combined with one nitrogen molecule.

Argon represents the greatest problem in formulating a theoretical model for a pumping mechanism. It does not combine chemically, and it does not penetrate deeply. Much attention has been given to the energetic backscatter theory[8]. By this theory, the part of the bombarding ion beam, which leaves the cathode as energetic neutrals, becomes buried in another surface. Sigmund[9] has investigated the question of the energetic processes which occur at a surface which is bombarded by keV ions whose masses match the target atoms. He concludes that only 2.5% of the energy is carried away from the surface. Correlating this result with sputtering yields demonstrates that most of the particles leaving the surface, both sputtered and backscattered, must leave a very low energy. There is evidence, however, that some small fraction of the incident particles can leave with a significant fraction of their incident energy. The energetic backscatter theory is supported by the fact that increased argon pumping speeds are observed when one cathode is replaced by tantalum. Tantalum is similar to titanium, being in the adjacent column of the periodic table, except having a heavier atomic weight. Elastic scattering theory[10] can be used to calculate the maximum backscattered energy that a particle can have after a single elastic collision. This energy is:

$$\frac{E_o}{E_i} = 1 - \frac{4\,M_1 M_2}{(M_1 + M_2)^2}$$

$E_o$ = backscattered energy

$E_i$ = incident ion energy

$M_1$ = mass of incident particle

$M_2$ = mass of target particle

Table 2-2 shows that in the case of argon, the tantalum cathode does allow single scattering events resulting in energetic backscatter. In the case of helium, the cathode material makes only a small difference.

TABLE 2-2

Fraction of Incident Energy Retained by a Particle
After a Single Elastic Backscatter Event

| | $H_2$ (2 AMU) | He (4 AMU) | Ar (40 AMU) |
|---|---|---|---|
| Ti (48 AMU) | 0.85 | 0.72 | 0.01 |
| Ta (181 AMU) | 0.96 | 0.92 | 0.41 |

It might be suggested that the true mass of an atom bound in a crystal lattice would be different than the free mass of the atom. This problem has been investigated by various workers, and they conclude that for the energy range below 10 keV, no "effective mass" is necessary to explain the observed phenomena[11]. Apparently the lattice binding forces are weak enough that the free

mass of the atom can be used. Also, the collision time, $10^{-16}$s is short compared to a lattice vibration. Indeed, there is available an analytical instrument called an "ion scattering spectrometer" which investigates the composition of solid surfaces based on this energy transfer equation[12].

We end up with a model for argon pumping in which 1% or less of the incoming atoms can leave as neutrals with a significant fraction of their incoming energy. This fraction, according to Sigmund, may be doubled and the maximum energy increased by changing to a tantalum cathode. Using an overall figure of 1-1/2% pumped atoms per ion, we can calculate a pumping speed of 0.08 liter/second from the results of Table 2-1. This model, however, is very quantitative, since only a small fraction of the incident energy would still represent an energy considerably above thermal, enabling the argon atoms to penetrate a few atomic layers in the anode, and be retained long enough to become buried by subsequent sputtering.

The energetic neutrals hypothesis has also been mentioned as a mechanism for pumping helium. However, in view of the above discussion and the results of Table 2-2, it appears that the scattering model does not work well for this combination. Experimental work by Anderson[13] et. al. indicates that less than 1% of the energy of a bombarding helium beam is reflected. This is explained by the deep penetratio, and the fact that most of the energy is deposited far below the surface. Replacing one titanium cathode with tantalum would be expected to have less effect on helium pumping than it does on argon because the model for helium-tantalum bombardment also indicates negligible sputtering ratios, and only slightly smaller penetration depths. The general conclusions derived from the helium-titanium model remain unchanged.

To summarize the pumping model for these four gases, we list in Table 2-3, the calculated speeds based on 100% burial of the ions formed in the case of hydrogen and helium, one nitrogen molecule combining with each sputtered titanium atom, and 1-1/2% of the argon atoms being pumped by energetic backscatter burial. Again the ion production rate is from Table 2-1.

TABLE 2-3

Results of Theoretical Pumping Speed Caculations

| | $H_2$ | He | $N_2$ | Ar |
|---|---|---|---|---|
| Theoretical Pump Speed $\ell/s^{-1}$-cell$^{-1}$ | 1.56 | .58 | .89 | .08 |
| Percent of Nitrogen Speed | 175% | 65% | 100% | 9% |
| Ultek D-I Pump Data[14] | 180% | 30% | 100% | 24% |

Comparing this pumping model with manufacturers specifications shows a good prediction of the hydrogen/nitrogen ratio. The helium value is high and argon is low. In view of the qualitative nature of the model, however, overall agreement is good.

Looking again at the model of hydrogen and helium pumping by penetration in the cathode, we do see that hydrogen penetrates deeper. Furthermore, hydrogen is soluble in the metal and has a very high diffusion rate. Helium, while it penetrates deeply does not further diffuse at normal temperatures. One would anticipate that penetration would be more efficient and complete for a fresh metal surface, then, as the pumping proceeded the easily available sites would become filled causing the pumping speed to drop, and previously pumped atoms to be re-emitted. There is evidence that most of the helium leaving the surface are atoms that have been "replaced" by incoming ions[15]. This experiment is done by exposing the surface first to $He^3$, then changing to $He^4$, and monitoring the products with a mass spectrometer. Thus, making adjustments for these differences in hydrogen and helium, it appears that cathode burial is the most likely pumping process. When the gas load consists entirely of these light gases, there is no significant sputtering, and the cathodes continue to take on the gases with a slower speed as the most available sites get filled. Speed and total loads for hydrogen are higher because of hydrogen's high solubility and diffusion constant. This model shows very clearly that the similarities between hydrogen and helium (light atoms) shed more light on the pumping process than the similarities between helium and argon (inert atoms).

Many pump modifications have been suggested for better pumping of argon with incidental comments that these modifications would also improve helium pumping. One of these is the triode pump[16]. In the triode pump, an additional screen cathode is inserted in the space between the anode and the plane cathode. The explanation for the increased argon pumping speed for this geometry lies in the fact that the impact at the screen cathode can be a glancing incidence. Such a scattering event has a higher cross section and leaves the energetic neutral with more energy. In view of the above model for helium pumping, it does not appear likely that the triode pump will significantly increase the pumping speed of helium. Instead, modifications to geometry and materials should be directed toward making the helium act more like hydrogen, i.e., choosing a cathode material with deeper penetration and higher diffusion constants.

If the surface processes can be modified to pump the helium ions as efficiently as they pump the hydrogen ions, then the model summarized in Table 2-3 shows that helium pumping speed could be as high as 30 percent of the hydrogen speed, instead of 10 percent as in commercial pumps. Such a pump would be expected to be slower pumping the heavier gases, but these are of less importance in the Jupiter mission. Pump modifications directed toward high helium speeds and constant helium and hydrogen speeds are discussed in Section 5.

# 3. SPUTTER ION PUMP TESTS

## 3.1 TEST OBJECTIVES

The objectives of the sputter ion pump tests were to obtain pumping speed data on pure gases and mixes that can be used to quantify the pump influence on a Jupiter atmosphere probe mass spectrometer, test the proposed model for pumping these gases, and indicate any modifications that may be required to meet the mission goals described in Section 1. The gases and mixes used in the tests are hydrogen, helium, nitrogen, argon, and a 90% hydrogen and 10% helium mixture.

Since it was anticipated that hydrogen would pump ten times faster than helium, a special objective of the tests on mixes was to determine if the presence of hydrogen affected the speed of the pump for helium. Also, since the mission is to last less than thirty minutes, the tests stressed the speeds as function of time, and particularly the ratio of the speeds as function of time. Speeds were measured as function of ion pump anode voltage and gas load. Finally, the background residual gas spectrum was measured with and without a gas load in order to quantify the effect of the pump on trace gas measurements in the Jovian atmosphere.

## 3.2 TEST PUMP AND APPARATUS

The test pump, Figure 3-1, was a special flight design, first developed for the Skylab Metabolic Mass Spectrometer[17]. It is an eight-cell diode pump with one titanium and one tantalum cathode, having a nominal pumping speed of four ℓ/s. Total weight including the magnet is 1.5 kg. The magnetic field at the gap center is 1100 gauss, and the operating voltage for the Skylab application was 4800 V. The pump represents a good departure point for the hydrogen-helium pumping studies.

The pumping speed test apparatus is shown in Figure 3-2. It is of the two-gauge calibrated conductance type[18]. It is constructed entirely of 1-1/2" bakable stainless components.

The mass spectrometer is a Varian quadrupole gas analyzer, Model 978-1000, having a mass range 1-100 AMU with detectible limit of $0.05 \times 10^{-9}$ torr for the partial pressure of any one peak. The auxiliary vacuum system consisted of a 20 ℓ/s ion pump with sorption roughing module for initial pump-down. Design considerations of the test apparatus can be related most easily to a brief description of pump speed measuring procedure.

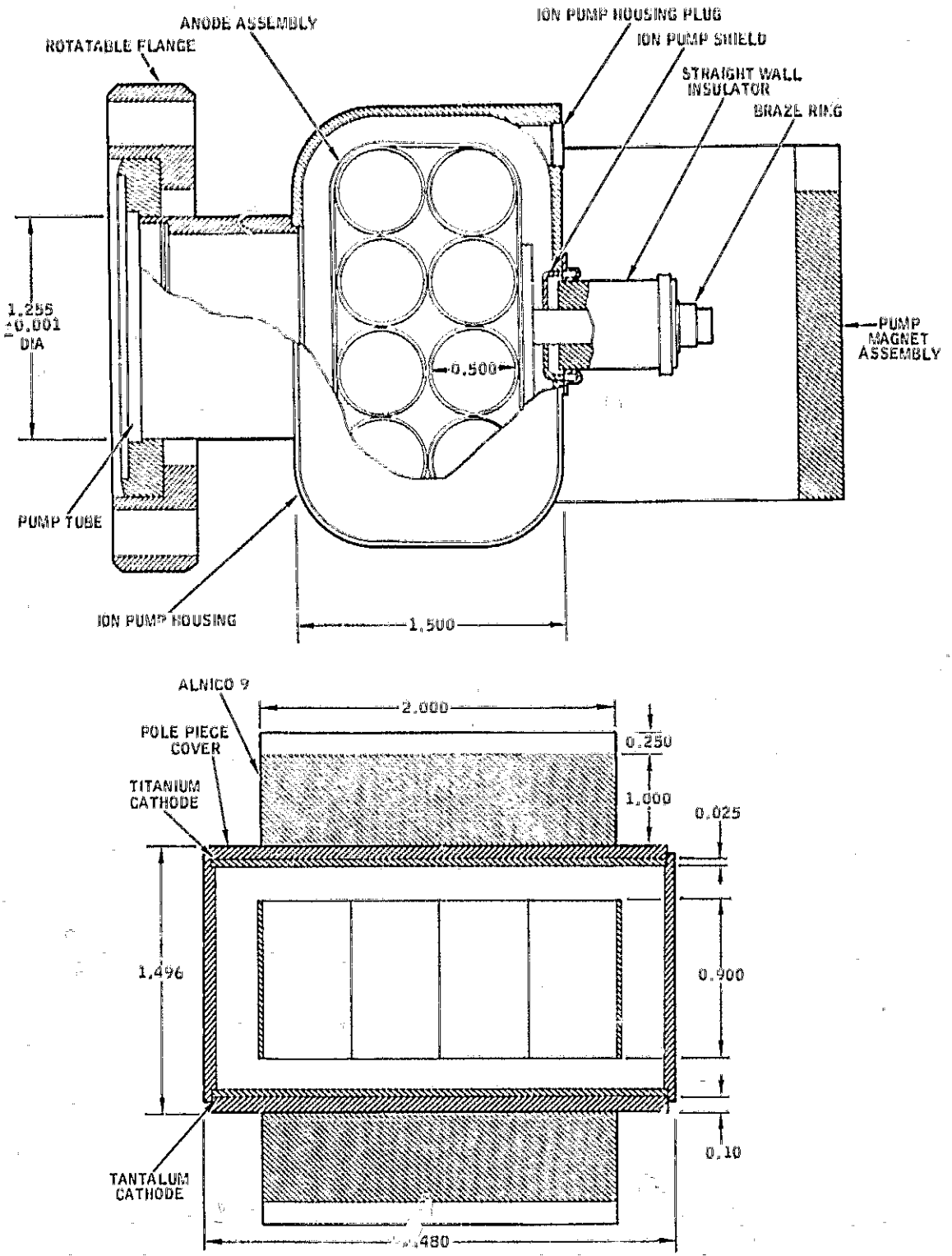


FIGURE 3-1

Eight Cell Prototype Ion Pump. This Pump is the Design Used With the Skylab Metabolic Mass Spectrometer

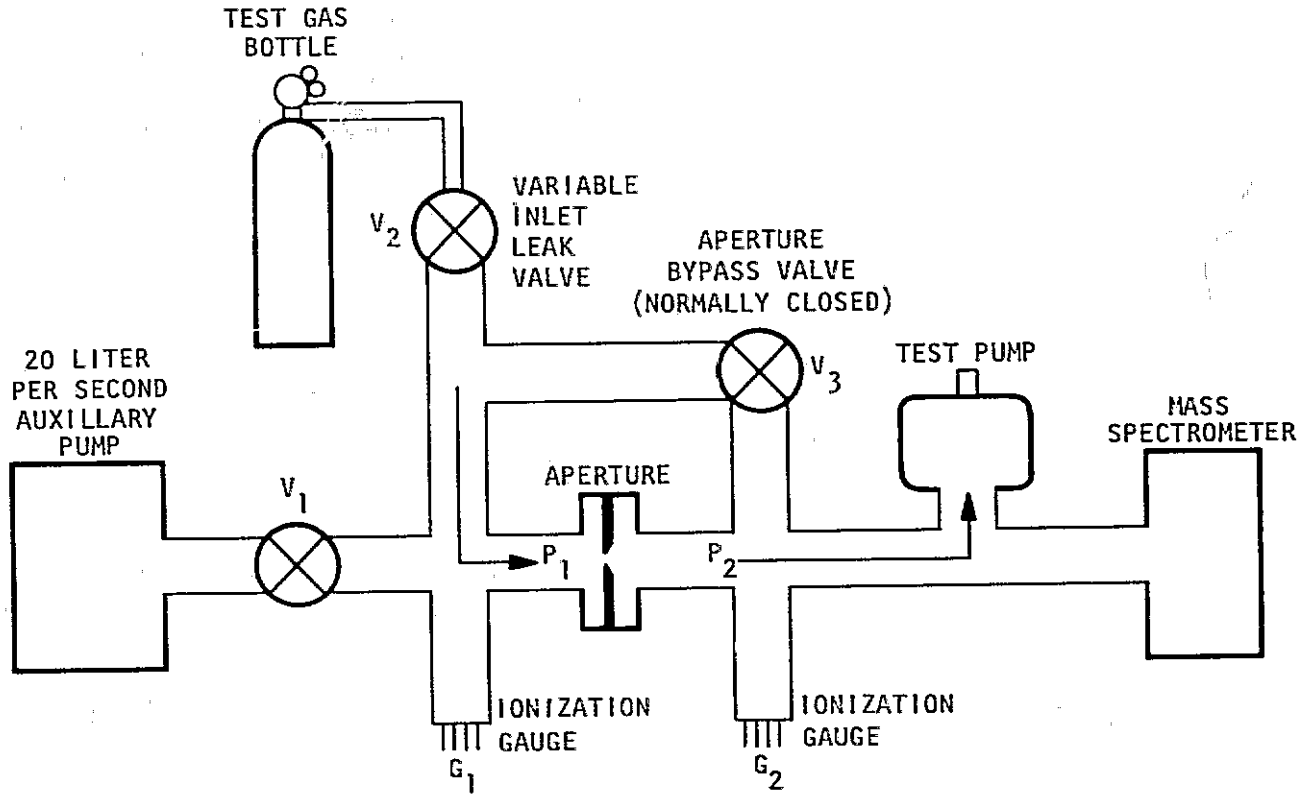


FIGURE 3-2

The System is Constructed of 1.5 Inch Bakeable Stainless Parts.
Conduction of Connecting Parts is Therefore in Excess of 100 Liters per Second in Each Case

To measure pumping speed, the test gas is admitted at the leak valve $V_2$, with valves $V_1$ and $V_3$ closed. The flow into the pump, Q, is then measured by the pressure drop across the calibrated conductance aperture.

$$Q = (P_1 - P_2)C = SP_2$$

Where $P_1$ and $P_2$ are pressures on the high and low side of the leak respectively, and C is the aperture conductance. S is the pumping speed of the pump at the pressure $P_2$. Solving for S,

$$S = (P_1/P_2 - 1)C$$

This relation illustrates that knowledge of the absolute pressure is not necessary since pumping speed is a function of the pressure ratio only. The relation is quite simple, all that is required is two pressure gauge measurements, and a measure of the calibrated conductance aperture. However, in practice certain complications arise, and the peculiarities of hydrogen and helium tend to emphasize some of the problems. Hydrogen, because it is pumped to a significant extent by the ionization type pressure gauges, and helium because the gauges are relatively insensitive to it, making pressure measurements less accurate.

The problems become most critical when testing the pump on the 90% hydrogen, 10% helium mix. In this case, with the helium pumping speed low by a large factor, the gauges being insensitive to helium by another factor, and the partial pressure of helium in the mix at only 10% of the total, the tests become very insensitive to changes in the helium pumping behavior. In order to extract the helium pumping speed from the data in the presence of hydrogen, the relation $S = (P_1/P_2-1)C$ must be used with the helium partial presures only. The partial pressures in the pump could be found by calibrating the mass spectrometer, but there was no way to obtain the partial pressures on the high pressure side of the aperture without a second mass spectrometer. Several possible ways of reducing the data were studied, and it was proved that without a second mass spectrometer it is impossible to obtain the helium pumping speed independently, but only as a ratio to the hydrogen pumping speed. The data reduction technique which is most sensitive to the helium speeds, described in Section 3.3.3, utilizes the calibrated mass spectrometer and the known concentrations of the sample gas in the bottle. The gauges and calibrated conductance are not required to reduce the data on mix pumping in this way.

Because of the complications of gauge pumping of hydrogen and low sensitivity to helium, many of the tests had to be repeated with increased emphasis on the mass spectrometer data before meaningful results could be obtained.

The general basis of the mechanical design of the system follows the principles described in reference 18. This means that the test pump is mounted on a side tube so that the molecules passing through the aperture must make one or more wall collisions before entering the pump. This arrangement is in contrast to those where the aperture is mounted on the mouth of the pump allowing streaming into the pump and giving artifically high speeds. The conductance of this side tube must be accounted for, but it is sufficiently large that corrections are less than 3%.

The choice of aperture size for the calibrated conductance represented a compromise in order to satisfy all of the goals of the experiment with one apparatus and avoid disassembling between runs. Anticipating seven ℓ/s hydrogen pumping speed, four ℓ/s nitrogen pumping speed and 0.7 ℓ/s helium pumping speed, an aperture was chosen with a helium speed of about 0.25 ℓ/s. This aperture results in a $P_1/P_2$ pressure ratio of approximately four for helium, 40 for nitrogen and 20 for hydrogen. A smaller aperture would give more accurate helium speed data with pure gas but would limit the highest allowable pump pressure for hydrogen speed tests to the middle of the $10^{-5}$ torr range. The aperture size is found from the desired conductance by the relation[19]:

$$C = 11.6\ (28.7/M)^{1/2}\ A$$

where A is the aperture area in square centimeters.

For the 0.039 in. hole used in these tests, the exact conductance is:

$C$ = 0.338 ℓ/s for $H_2$

0.239 ℓ/s for He

0.0903 ℓ/s for $N_2$

0.108 ℓ/s for Ar

A small additional correction factor can be made when the plate containing the hole is contained in a larger tube [19]. For this apparatus this correction is less than 1% and so is ignored.

## 3.3 TEST PROCEDURE

### 3.3.1 Pumping Speed Tests of Helium, Nitrogen and Argon

Before measuring the pumping speeds of the pure gases, the system was baked overnight at 250°C with the aperture bypass valve open, the test pump on, and the auxiliary vacuum system open to test region. The gauges were then outgassed, with the auxiliary vacuum pump still open. Next, gauge tracking was tested by closing the auxiliary vacuum pump and leaking the test gases in one at a time, still with the aperture bypass valve open. The gauges were found to read the same within 3% over the pressure range $2 \times 10^{-7}$ torr to $2 \times 10^{-5}$ torr for each gas. The aperture bypass valve was then closed, and the test gas introduced through the leak. Gauge pumping was checked by monitoring the test gas with the mass spectrometer and turning the gauges on and off. Mass spectrometer pumping was likewise checked by monitoring with the gauges and turning the mass spectrometer filament on and off. No perceptible pumping of the mass spectrometer or gauges could be observed for the helium, nitrogen, or argon samples.

The tests then proceeded by noting the background pressures and pump current with the leak valve closed. Opening the leak valve, the two pressures and the pump current under load were recorded. The speed was calculated by the relation

$S = (P_2/P_1 - 1)C$ using the pressures corrected for background, and using the appropriate value for the calibrated conductance for helium, nitrogen, and argon. To relate the pump gas load pressure gauge reading, $P_2$ to the true pressure in torr, the manufacturers gauge correction factor was used[22]:

Gauge Multiplier: 6.22 for helium

1.0 for nitrogen

0.84 for argon

This was the basic procedure used. Tests were repeated with various gas loads, times, voltages, and with different processing to the pump between loads. Processing details and results are presented in Section 4.

3.3.2 Pumping Speed Tests on Hydrogen, Gauge Pumping

When the test procedures, used for the other gases, were used for hydrogen, it was discovered that the gauges did pump hydrogen to a significant degree. It was not possible to accurately measure the pumping speed, but indirect evidence indicated hydrogen pumping speeds of 0.5 - 1.0 ℓ/s by the gauges.

Gauge pumping is a well known phenomenon. Dushman[21] refers to several studies indicating that much of the pumped gas in an ionization gauge is collected at the walls in glass gauge tubes. Furthermore, the pumping is more efficient if there is a thin coat of metal on the glass walls. In the apparatus used in these tests of course, the gauges are nude and contained directly in the metal system. Perhaps the metal walls are the reason that significant hydrogen pumping was observed in our system while none was observed in University of Michigan study[1] where glass gauges were used.

The gauge pumping is proportional to the emission current, so one method of reducing it, is to reduce the emission to some low value, and recalibrate the gauges accordingly. The emission was automatically reduced, and the calibration built in, on the Varian 971-1008 controller when the higher pressure ranges were used. Manufacturers literature on the controller specifies:

| | |
|---|---|
| $10^{-4}$ torr range | 30 μA emission current |
| $10^{-5}$ torr range | 300 μA |
| Lower ranges | 4 mA |

Checking gauge pumping on the $10^{-5}$ and $10^{-4}$ torr ranges disclosed that these ranges did not pump to a measurable degree. Further tests showed that the mass spectrometer did not pump hydrogen, so it was decided to calibrate the mass spectrometer hydrogen peak height against the gauge pressure. Thus, the following procedure was adopted: the high pressure side of the conductance aperture was measured on the gauge $P_1$, keeping it on the $10^{-5}$ torr range. The low pressure pump side of the aperture was measured with the gauge $P_2$ off, using the calibrated mass spectrometer. Pressure data for the calibration utilized the gauge factor from the Varian literature to convert apparent gauge readings to pressure in torr[20]:

Gauge Multiplier - 2.0 for hydrogen

With the calibrated conductance, C, of 0.338 ℓ/s for hydrogen, the pressures, again corrected for background, are used in the relation $S = (P_1/P_2 - 1)C$ to find the hydrogen pumping speed for various loads, times, voltages, and after various processes. Data on the mass spectrometer calibration and pumping speed results are presented in Section 4.

Another method of dealing with the problem of gauge pumping is suggested by Dushman[19]. Although not used in the present study, it is mentioned here for completeness. Since the gauge can be very fast responding, compared to pumping time constants of the apparatus, good pressure measurements can be made by operating the gauge very briefly and noting the value before it has a chance to alter the pressure by its own pumping action. To do this, the gauge filament must be continuously heated, and the gauge turned on and off by the tube voltages. Without applied voltages, there is no filament emission and hence no ionization.

### 3.3.3 Pumping Speed Tests on 90% Hydrogen and 10% Helium

The gauge pumping that was observed for pure hydrogen was also observed when pumping the mix. The same method was used to resolve the problem, i.e., by calibrating the mass spectrometer. Since the gauge measuring the pump pressure had to be off because of hydrogen pumping, the mass spectrometer was calibrated for helium partial pressures as well.

As mentioned previously, it is not possible to obtain the pumping speed of helium in the presence of hydrogen without an additional mass spectrometer on the high pressure side of the conductance aperture. Since this was not available, two methods were used to deduce the ratio of the pumping speeds from the available data. The first method used the following logic:

a. From the mass spectrometer readings and the calibration data, the true pressures at the pump were determined.

b. From the assumed pumping speed for hydrogen, and the known conductance, the partial pressure of hydrogen on the upstream side of the aperture was calculated.

c. With the appropriate gauge correction factors, the reading on the high pressure side could be separated into its hydrogen and helium components.

d. With helium pressures on each side of the conductance found in this way, the helium pumping speed can be calculated.

Applying this method to a few test runs demonstrated that it was very insensitive to changes in the pumping of helium because of the low sensitivy of the gauge to that gas. This method was therefore abandoned in favor of the one described below.

Assuming the known ratio of the gases in the sample bottle, the ratio of the hydrogen flow $Q_{H_2}$ to the helium flow $Q_{He}$ is given by:

$$\frac{Q_{H_2}}{Q_{He}} = \frac{P_{H_2}}{P_{He}} \quad \frac{C_{H_2}}{C_{He}} = \frac{P_2{}^{H_2}}{P_2{}^{He}} \frac{S_{H_2}}{S_{He}}$$

Where $C_{H_2}$ and $C_{He}$ in this case are the conductances of the leak valve. Assuming molecular flow, and using the manufacturers ratio of the pressures of the gases in the bottle (9.53), we have:

$$\frac{S_{He}}{S_{H_2}} = \frac{1}{9.53\sqrt{2}} \frac{P_2{}^{H_2}}{P_2{}^{He}} = 0.0742 \frac{P_2{}^{H_2}}{P_2{}^{He}}$$

Note that the calibrated conductance is not used in this relation, the gauges are not used, and the aperture bypass can be open or closed.

# 4. TEST RESULTS

## 4.1 MASS SPECTROMETER CALIBRATION

The results of calibrating the quadrupole mass spectrometer peak against the gauge reading for hydrogen and helium is shown in Figure 4-1. By applying the gauge multiplier, the true pressure is shown for each gas. The ratio of the calibrations is shown in Figure 4-2, for convenience in measuring the ratio of the pumping speeds.

## 4.2 PUMPING SPEEDS-STEADY STATE

Steady state pumping speeds for hydrogen, helium, nitrogen and argon are shown in Table 4-1. Also shown are the experimental values for the discharge intensity and the pumping efficiency in atoms pumped per ion in the discharge.

TABLE 4-1

Steady State Pumping Speeds, Discharge Intensities, and Pumping Efficiencies

| Parameter | $H_2$ | He | $N_2$ | Ar |
|---|---|---|---|---|
| Pumping Speed ℓ/s at $10^{-6}$ torr | 2.9 | 0.6 | 2.1 | 0.4 |
| Discharge Intensity amp-torr$^{-1}$ | 24.6 | 9.71 | 29.5 | 59.7 |
| Pumping Efficiency Molecules ion$^{-1}$ | 0.68 | 0.35 | 0.40 | 0.04 |

With the exception of helium, these results could be reproduced with the pump after a 16 hour bake at 250°C with the pump operating and open to the auxiliary vacuum system. They represent a steady state speed which is achieved after 20-30 minutes. Helium, as discussed below, was more dependent on pump treatment. Comparing these results with the pumping model presented in Section 2, shows that there is a qualitative comparison, with the ratios of the various speeds being somewhat as predicted. In the model, the discharge intensity was exactly proportional to the maximum in the ionization cross sections. Here, we find that discharge intensity does follow the cross section trends, but the ratios are somewhat different. The model, of course does not consider the energy distribution of the electron cloud, and the integral of the ionization cross section across this distribution, as well as other factors such as secondary electron production.

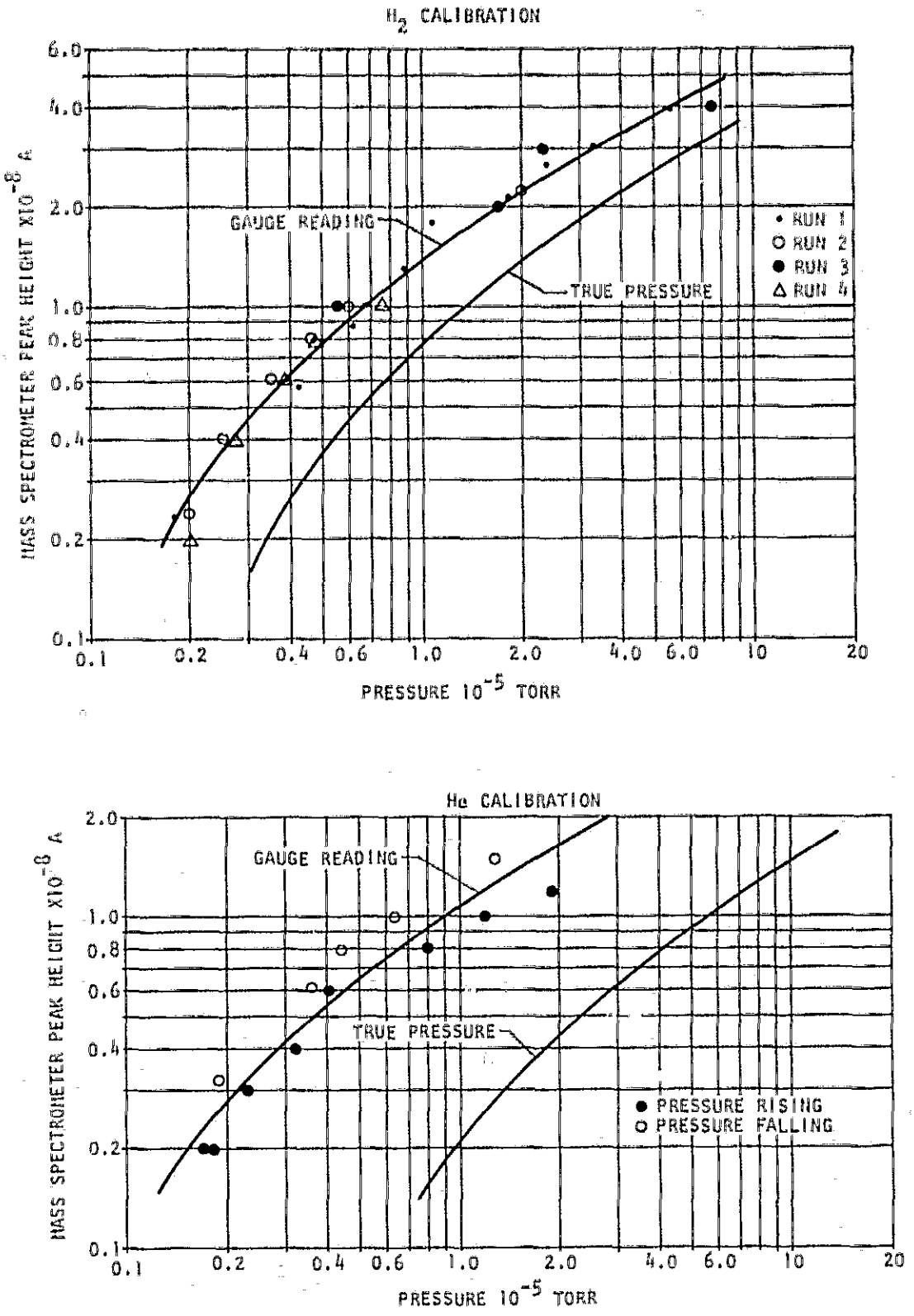


FIGURE 4-1

Calibration of Mass Spectrometer Showing Indicated Gauge and True Pressure

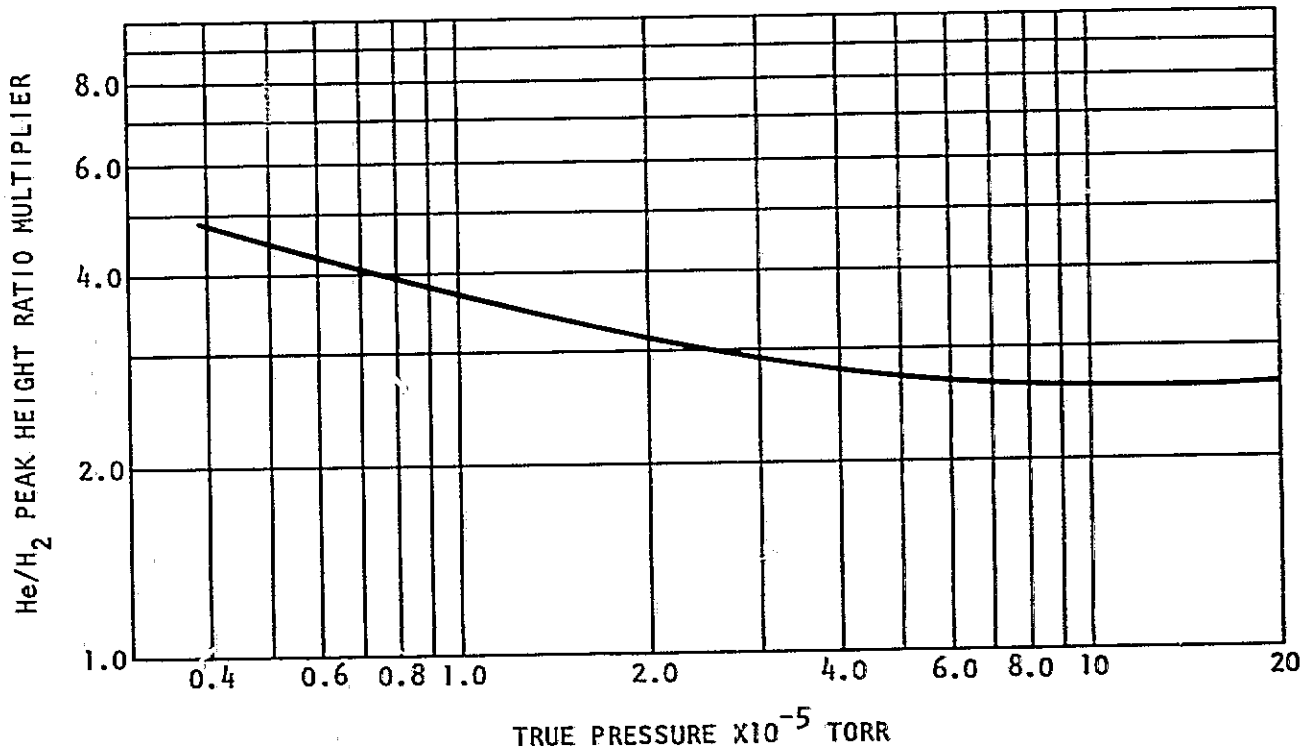


FIGURE 4-2

Ratio of Mass Spectrometer Calibration Factors from Figure 4-1

The nitrogen pumping speed is lower than the four ℓ/s which had been achieved by this pump design when it was used with the Skylab mass spectrometer. The normal discharge intensity for nitrogen in the Skylab application was 80 A-torr$^{-1}$ so the low discharge intensity observed in these tests is reflected in the low pump speed. After processing the pump by bake cycles, argon pumping, and higher voltages, the pumping speed for nitrogen did not increase, and it was concluded that the most likely cause for the low pumping speeds was in the magnet. The magnet was demounted and recharged, but the speed still did not increase. Nonuniformity may distort the electron cloud is some way. Since the discharge intensity affects ion production in all four gases by the same factor, the emphasis is therefore placed on pumping speeds normalized to the nitrogen value. Reducing the discharge intensity and the measured pumping speed to atoms pumped per ion in the discharge on the last line of the table shows again that the qualitative predictions are verified. Hydrogen is very efficiently pumped, but helium, with its higher mass, lower penetration, and negligible diffusion is not retained as well by the surfaces under bombardment. Argon pumping is somewhat higher than the model predicts, but in view of the lack of hard data on backscatter fraction and backscatter energy, the agreement is still quite good. The pumping efficiency results show again that argon stands alone in being very inefficiently pumped, because of it being inert and having only limited penetration in the cathode, resulting in the lowest pumping speed in spite of having the highest ionization cross section and discharge intensity. The low helium pumping speed, on the other hand is due largely to its low ionization cross section and low discharge intensity. Once the ions are formed, they are removed into the pump surfaces approximately the same as nitrogen and at about one-half the rate of hydrogen. The similarities in hydrogen and helium pumping processes are quite obvious by these results.

The helium pumping speed shown in Table 4-5 was not consistently reproduced. Several tests were made after the 250°C 16 hour bake only to find the helium pumping speed as much as a factor of 2 lower than the 0.6 ℓ/s. The discharge intensity was consistent within 10%, indicating that the problem is in the burial efficiency at the cathodes. The surface conditions are likely to exert a strong influence on the helium ion penetration depth. Since the highest pumping speeds are assumed to be associated with clean, outgassed surfaces, the pump treatments emphasized baking, loads of argon to sputter the cathodes, and overvoltages. Unfortunately, consistent results could not be achieved, indicating that more work in this area could be useful.

## 4.3 HELIUM AND HYDROGEN PUMPING SPEEDS, LOAD AND TIME DEPENDENCE

The pumping speeds of both hydrogen and helium always started out at a relatively high value and decreased as the test progressed. According to our theoretical model, this is best explained by assuming that the most easily available sites for pumping become filled, limiting the cathode penetration for further pumping. According to this, it would be reasonable to plot the pumping speed as a function of the total amount of gas previously pumped. Hydrogen and helium pumping speeds for constant pump pressure are shown in this way in Figure 4-3. The helium data at two different pump pressures shows that the rate of pumping, as well as the total gas pumped, influences the

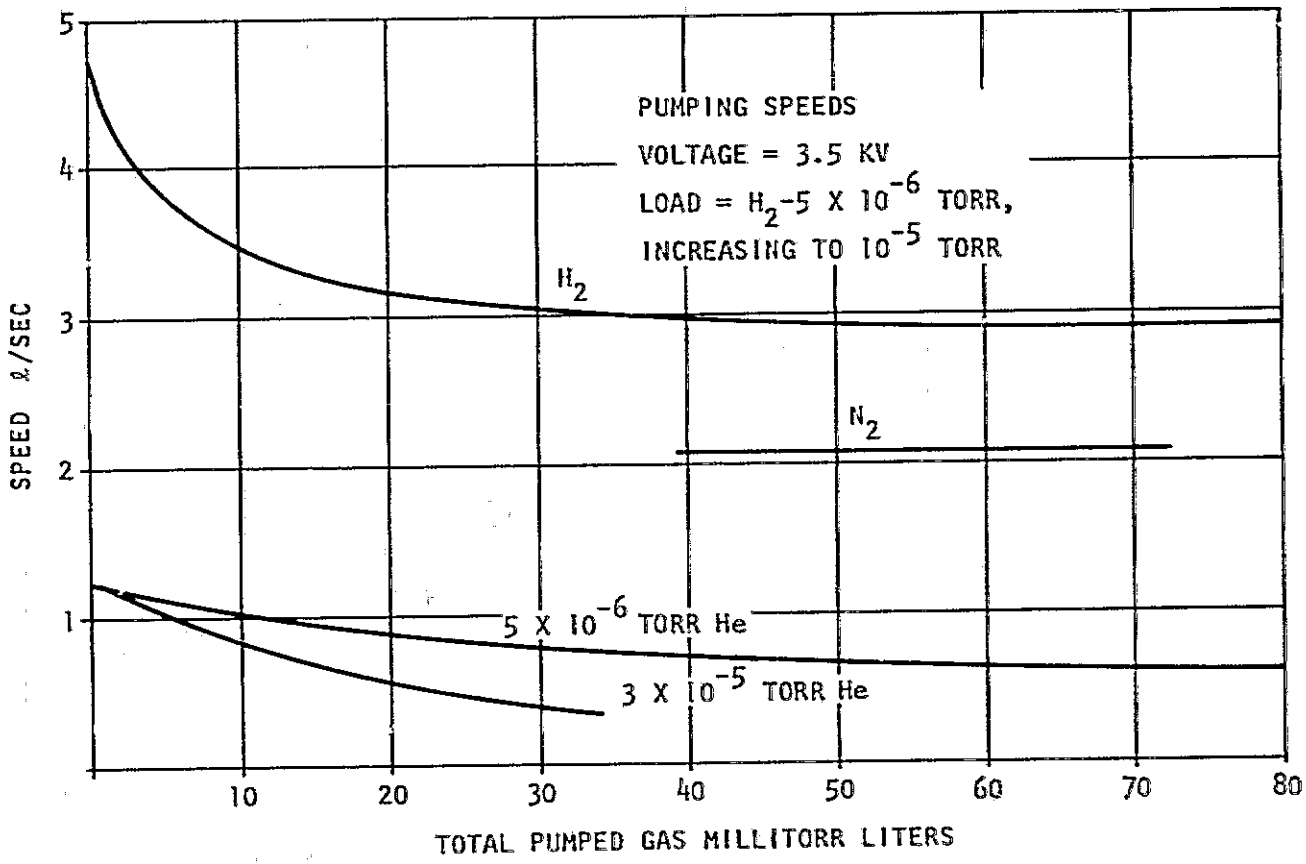


FIGURE 4-3

Typical Result of Pumping Speed of Pure Gases as Function of Total Load

pumping speed. The hydrogen pumping speed did not show this effect within the pressure range $5 \times 10^{-5}$ torr - $1 \times 10^{-6}$ torr. The higher diffusion coefficient of the hydrogen may cause this difference by allowing the pumped atoms to move out of the way more easily, making the sites near the surface repeatedly available.

Of more importance to the mass spectrometer application, is the ratio of the pumping speeds as a function of time. These tests received the prime emphasis. To increase the data rate over what could be recorded by hand, a strip-chart recorder was driven by the mass spectrometer output. The mass spectrometer was set to sweep from 2 AMU to 4 AMU each ten seconds. The recorder would then record the peak height ratios from the instant the test gas was admitted through the leak valve. A typical record is shown in Figure 4-4. The ratio of the peak heights on this strip chart, and the ratio of the quadrupole calibration factors, Figure 4-2, were used to calculate the ratio of the helium to hydrogen pumping speeds as a function of time.

The results, shown in Figure 4-5 indicate a very marked change in the ratio of the pumping speeds particularly over the first 100 seconds. This transient pumping speed is caused by the extremely high initial pumping of hydrogen. This initial pumping, as mentioned in Section 2, is probably not associated with any ionization of the gas in the discharge, but instead is related to direct absorption of hydrogen on the pump walls. This strong variation of speed with time may cause a larger calibration problem for the mass spectrometer than the low helium pumping speed.

## 4.4 PUMPING SPEED VARIATION WITH VOLTAGE

The variations of pumping speed with voltage on the hydrogen and helium test gases proved to be very difficult measurements to make. At first, the procedure for this test was adopted exactly as described for the steady state pumping measurements. A test of pumping speed at 3.5 kV would be made, then the voltage would be raised, leaving all of the other variables, such as the gas flow, constant. Values would be measured every 1000 V up to 9.5 kV, the gas flow would then be stopped, and the backgrounds at 9.5 kV noted. Observing that the high voltage background was different, the pump would be returned to 3.5 kV, where it was found that the low voltage background changed as well. Furthermore, rechecking the pumping speed at 3.5 kV disclosed that the pumping speed had also changed.

To resolve this difficulty, the testing procedure was modified to take background measurements at each voltage, as well as to measure the pumping speed at 3.5 kV after each measurement at higher voltages. The measurements were then normalized to the speed at 3.5 kV to separate the time effects.

As shown in Figure 4-6, the voltage coefficient of pumping speed is less than 5% for hydrogen and helium when the voltage is raised from 3 kV to 9 kV. The speed for nitrogen increases by 25% for this same voltage change. The discharge intensity did not vary with voltage for hydrogen and helium, so the pumping processes at the surface (pumping efficiency) are apparently constant.

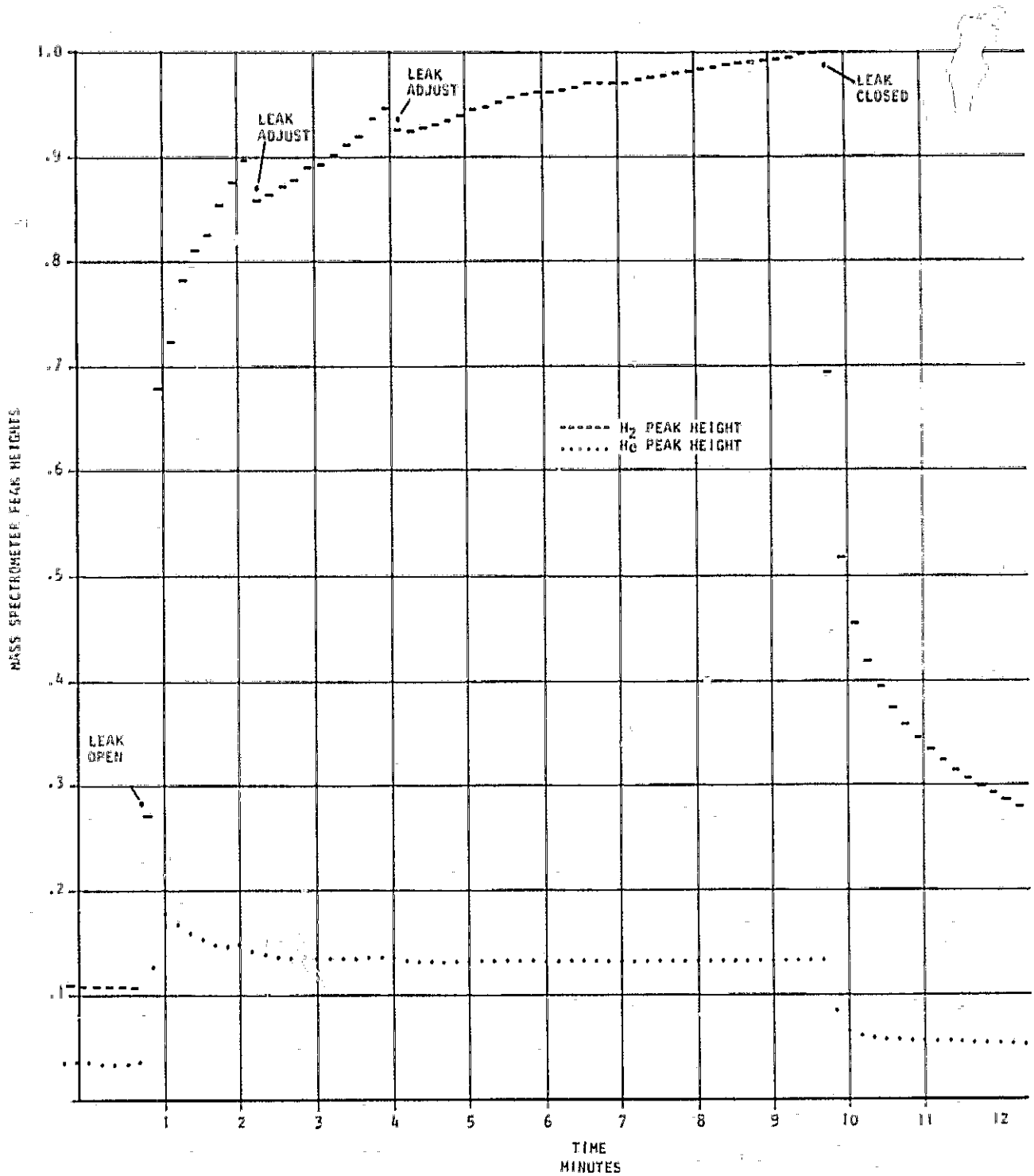


FIGURE 4-4

Recording of Mass Spectrometer Peak Heights for $H_2$ and He Every Ten Seconds While Introducing the $H_2$/He Mix

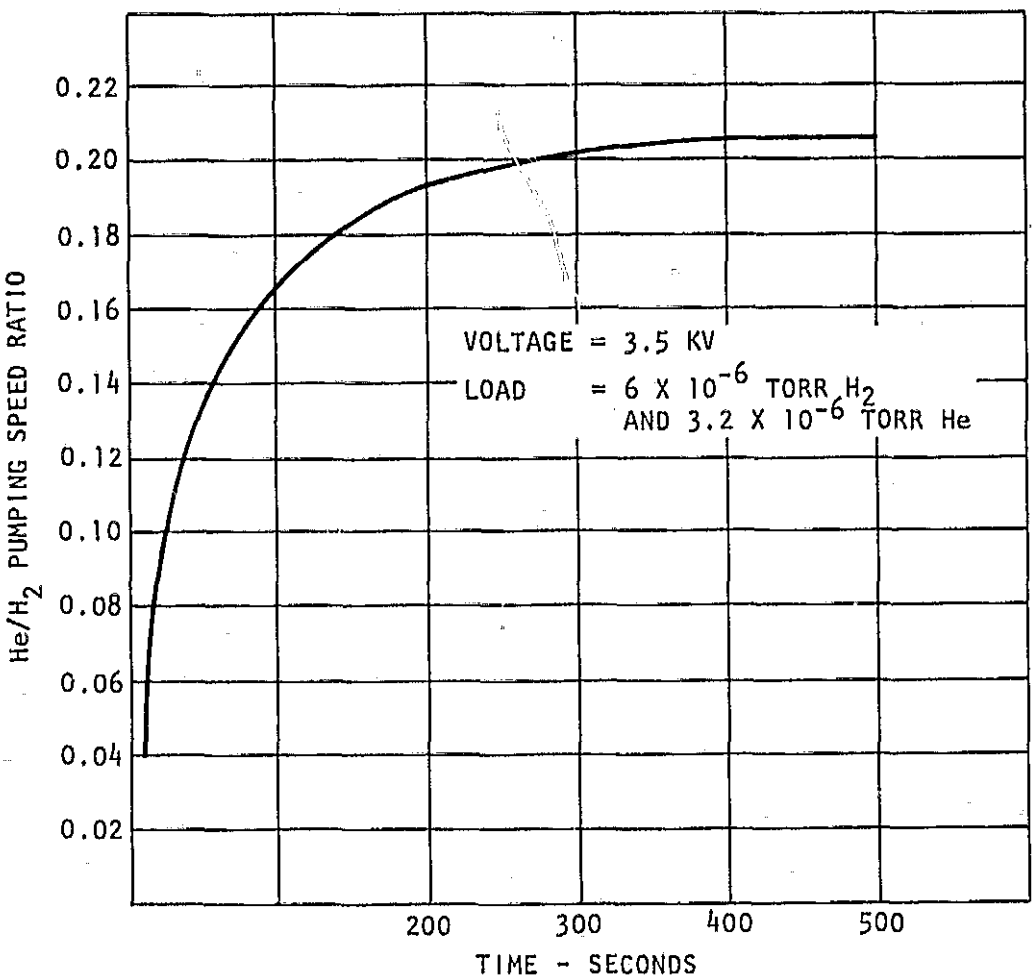


FIGURE 4-5

Typical Ratio of He to $H_2$ Pumping Speeds vs Time
The Change is Mostly in the $H_2$ Pumping Speed

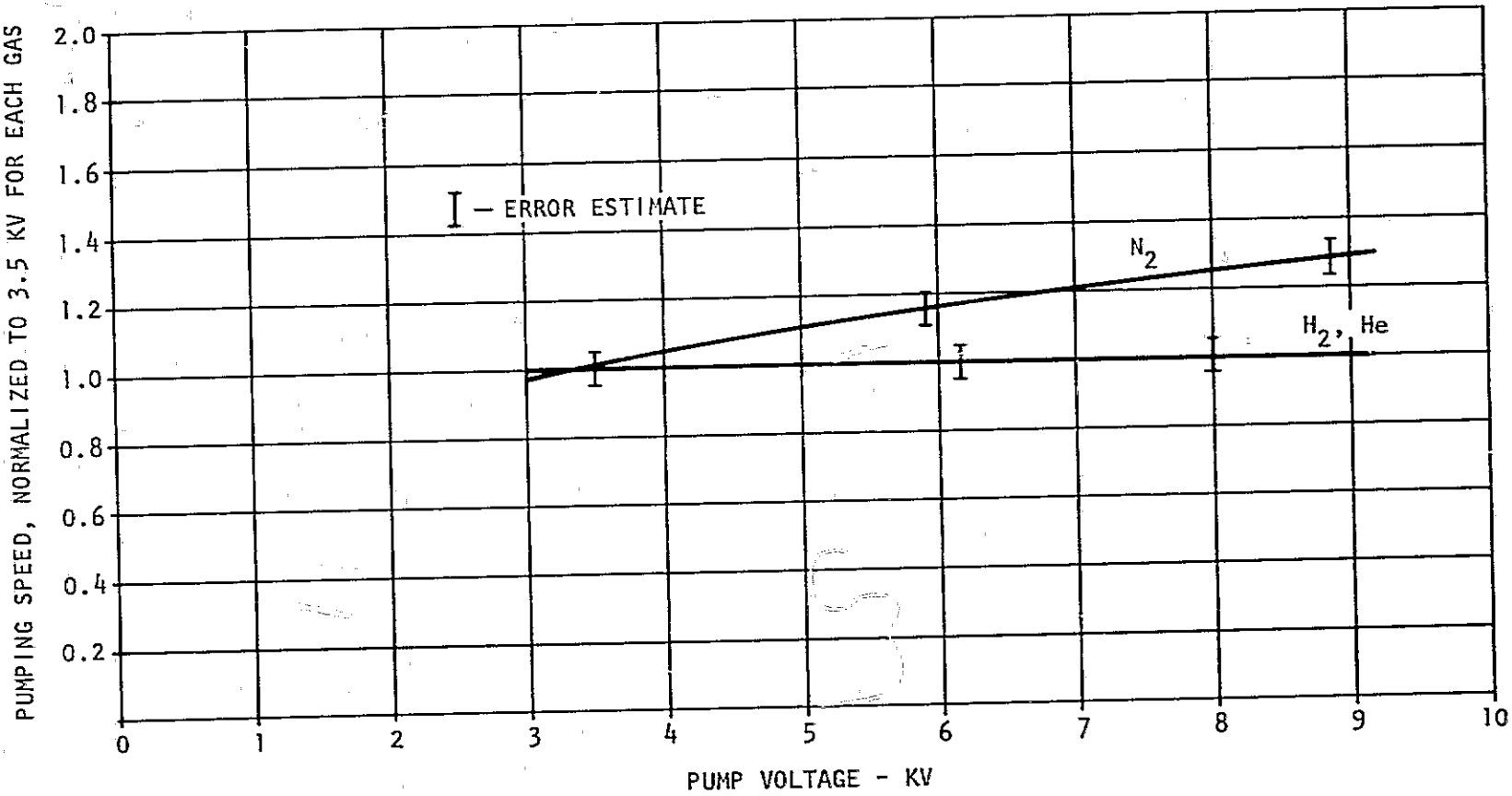


FIGURE 4-6

Voltage Dependance of Pumping Speed

Since the model of the electron cloud, presented in Section 2, indicates that the charge density and hence the discharge intensity should be proportional to voltage, the results shown in Figure 4-6 do not appear to support the model. Jepsen[20], however has shown that when the magnetic field is low, the voltage coefficient is less, and for a sufficiently low magnetic field, the pumping speed is independent of voltage. This effect is apparently related to the inability of the electrons to sustain a Townsend avalanche without the constraining effect of the magnetic field. Since the cross sections for hydrogen and helium are lower, the mean free path between collisions is longer, requiring a higher magnetic field to achieve the Townsend avalanche for these gases. Thus, the small variation with voltage for nitrogen and the lack of variation for hydrogen and helium may again be related to the same magnet problem that caused the low pumping speed.

## 4.5 RELATING PUMP PERFORMANCES TO MASS SPECTROMETER SOURCE PRESSURE

The goal of the tests presented in this report is to examine the influence of pump performance on the mass spectrometer source pressure. In Section 1 it was mentioned that the effect of the pump was reduced by the factor of the differential pumping ratio, the pump speed divided by the source conductance. With the two gases having different pump speeds and different source conductances, the effect becomes more involved. Note that the components of the pump test station, Figure 3-1, are completely analagous to the components of a mass spectrometer analyzer with a differentially pumped source. The leak, $V_2$, is the sample leak, the region $P_1$, is the source, the aperture is the source conductance and the test pump is the analyzer pump. Relating source pressures to pumping speeds therefore involves the same type of calculations shown above to determine pumping speeds.

The flow equation for helium and hydrogen from the sample gas to the pump is given by:

$$Q_{H_2} = C^L_{H_2} P^{H_2} = \left( P_1^{H_2} - P_2^{H_2} \right) C^S_{H_2} = P_2^{H_2} S_{H_2}$$

$$Q_{He} = C^L_{He} P^{He} = \left( P_1^{He} - P_2^{He} \right) C^S_{He} = P_2^{He} S_{He}$$

where

$Q_{H_2}$ = Flow of $H_2$ torr cc/s

$C^L_{H_2}$ = Sample leak conductance for $H_2$, cc/s

$P^{H_2}$ = Sample pressure of $H_2$, torr

$P_1^{H_2}$ = Source pressure of $H_2$, torr

$P_2^{H_2}$ = Pump pressure of $H_2$, torr

$S_{H_2}$ = Pump speed for $H_2$, cc/s

$Q_{He}$ = Flow of He torr cc/s

$C_{He}^{L}$ = Sample leak conductance for He, cc/s

$P^{He}$ = Sample pressure of He, torr

$P_1^{He}$ = Source pressure of He, torr

$P_2^{He}$ = Pump pressure of He, torr

$S_{He}$ = Pump speed for He, cc/s

Solving for the ratio of the partial pressures in the source, and eliminating the pressure at the pump, we have

$$\frac{P_1^{H_2}}{P_1^{He}} = \frac{P^{H_2}}{P^{He}} \frac{\left(1 + \frac{C_{H_2}^{S}}{S_{H_2}}\right)}{\left(1 + \frac{C_{He}^{S}}{S_{He}}\right)}$$

Where $C_{He}^{S}$ and $C_{H_2}^{S}$ are source conductance for helium and hydrogen respectively. Thus the ratio of the pressures in the source is the same as the ratio in the sample gas, except corrected by the factor (1 + C/S).

Assuming the source conductances for hydrogen and helium of 224 cc/s and 158 cc/s from the Skylab mass spectrometer source, the ratio of these correction factors is shown in Figure 4-7 for the range of pump speeds observed in the tests. From this figure we see that for a 1% precise measurement in the hydrogen/helium ratio, the speed for both gases must remain constant, or they must move together. The typical situation observed in the tests was that the helium speed would change more slowly, thus only partially offsetting the approximately 3% error caused by the hydrogen speed change from 5 ℓ/s to 3 ℓ/s. The helium speed, however, as discussed in Section 4.3 was not very repeatable from day to day. Without calibration, the uncertainty of helium speed could cause a ratio error of 10% or more in the source.

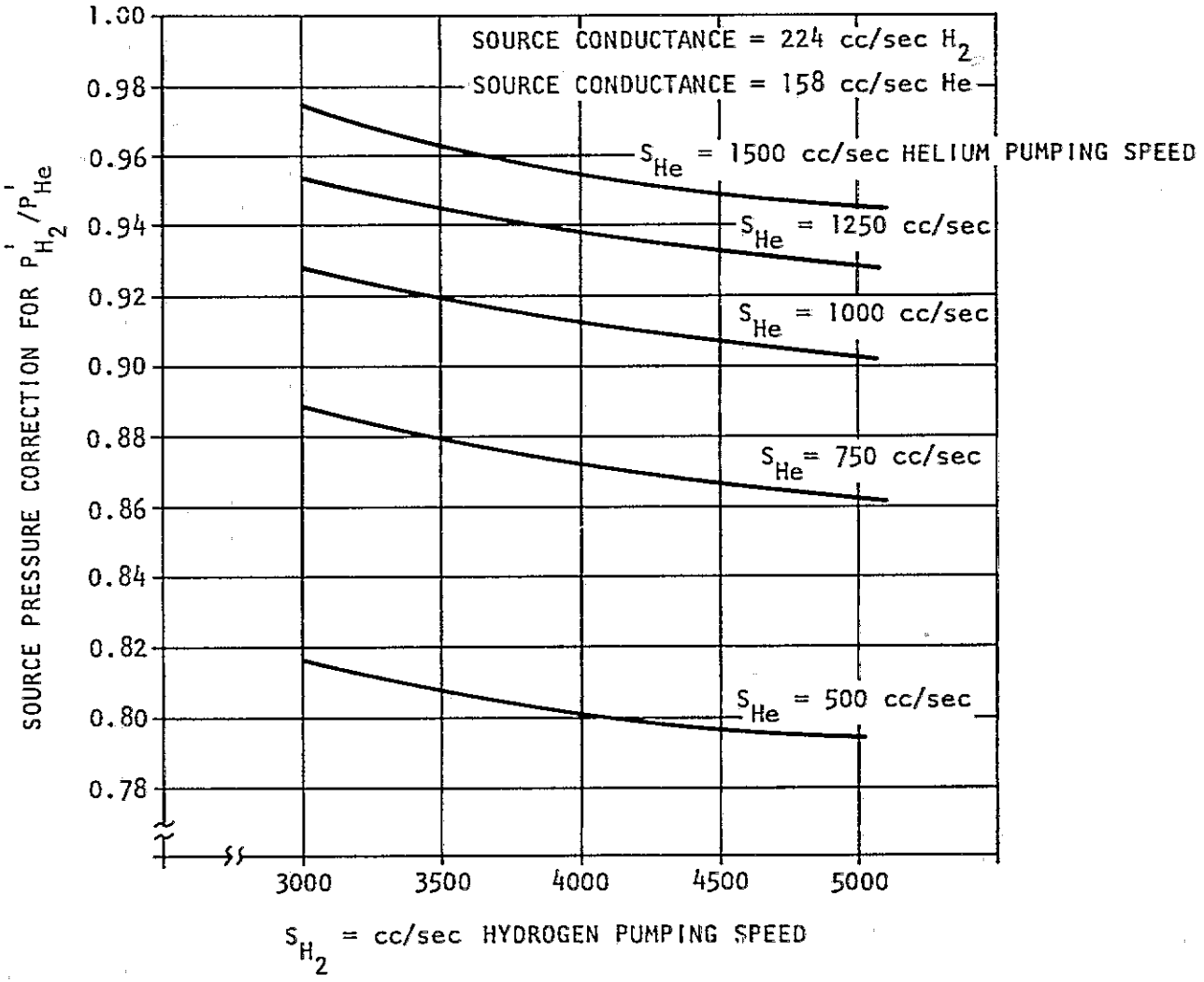


FIGURE 4-7

The Ratio of $H_2$/He in the Source Deviates from the Ratio $H_2$/He in the Sample Gas by the Factor on the Ordinate

## 4.6 BACKGROUND GAS AND MEMORY EFFECTS

The background and memory measurements were performed after a 16 hour 300°C bakeout. The bakeout temperature was limited by the mass spectrometer analyzer tube. With the auxiliary vacuum system shut off, and the bypass valve closed, the background spectrum at the pump was recorded over the mass range 2-52 AMU. Next, the hydrogen-helium sample mix was admitted to a pump current level of 100 μA and the entire spectrum was recorded again. The results are shown in Table 4-2.

Since the bakeout temperature was limited by the mass spectrometer tube, the ultimate pressure for these tests was $3.7 \times 10^{-7}$ torr. Increased temperatures and longer bakes would result in lower pressures, but these tests give a good measure of pump memory effects by comparing the spectra with and without gas load. If a gas did not increase with sample gas load, it was assumed it was a background gas associated with the system as a whole, and not necessarily generated in the pump. Such gases could certainly limit the detection of some of the trace constituents, but it is assumed that with improved pump processing, these gases could be reduced to a low pressure, enabling sensitive measurements to be made.

When a gas level increased with sample load, it was assumed that either the gas was being formed by interactions in the pump or it was being re-emitted, having been buried during some previous pumping history. It was impossible to separate these effects to know if additional pump processing could reduce the partial pressures. The only indication we could go by was the degree to which the partial pressures increased. If they increased a great deal, it is assumed that the sample gas is reacting in the pump or in the mass spectrometer source and forming new gases. If the gas increased only slightly, it was assumed that the gas is likely to be a memory of a previously pumped specie and that improved processing will likely reduce the effect.

Two gases stand alone as being definitely formed with the gas load. They are at 3 AMU, $H_3^+$, and 5 AMU. Under normal sample load the 3 AMU $H_3^+$ was evolved with a partial pressure of $6 \times 10^{-8}$ torr and the 5 AMU gas showed $2 \times 10^{-9}$ torr, approximately 1000 and 100 times higher than background respectively. These products will cause an interference in measurements of the Jovian atmosphere at about the $6 \times 10^{-4}$ level and $2 \times 10^{-5}$ level. The gas at 5 AMU is not mentioned by Kennedy[1] as an important species on Jupiter, but 3 AMU is expected, due to $He^3$ and HD, at a total mixing level of $10^{-4}$. With the pump product measured here, this particular level on Jupiter will be difficult or impossible to measure. measure.

Other gases evolved by the pump to a significant degree are shown in Table 4-3. They are classified as gases whose partial pressure increased by a factor of 10 or more when the sample gas was introduced.

The gas found at 17 AMU is possibly $NH_3$. This gas forms clouds at the 1 bar level in the Jovian atmosphere. The level of the gas from the pump found in these tests will cause a severe interference with this measurement. Since 28 AMU is a strong background due to testing the pump with nitrogen, it is likely that the previously pumped nitrogen is influencing the formation of $NH_3$. One goal of future tests should be to determine if excluding nitrogen from the pump from its initial fabrication would limit the formation of the gas at 17 AMU.

TABLE 4-2

Background and Memory Spectra

| Mass AMU | Background Peak Height | Peak Height with 10% He, 90% He Gas Load at I=100μA |
|---|---|---|
| 2 | $150 \times 10^{-12}$ A | $7000 \times 10^{-12}$ A |
| 3 | 0.15 | 130.0 |
| 4 | 12.0 | 720.0 |
| 5 | <0.03 | 5.0 |
| 7 | 0.03 | 0.03 |
| 12 | 1.0 | 2.0 |
| 13 | 0.15 | 1.5 |
| 14 | 32.0 | 35.0 |
| 15 | 2.0 | 20.0 |
| 16 | 4.0 | 40.0 |
| 17 | 3.0 | 35.0 |
| 18 | 6.5 | 52.0 |
| 19 | 0.4 | 3.0 |
| 20 | 6.0 | 10.0 |
| 22 | 0.12 | 0.2 |
| 24 | 0.03 | 0.15 |
| 25 | 0.1 | 0.45 |
| 26 | 0.7 | 3.0 |
| 27 | 2.0 | 7.0 |
| 28 | 400.0 | 400.0 |
| 29 | 5.0 | 50.0 |
| 30 | 1.0 | 2.0 |
| 32 | 7.0 | 5.0 |
| 33 | <0.03 | 0.3 |
| 34 | 0.03 | 0.4 |
| 35 | 0.25 | 0.45 |
| 36 | 1.0 | 3.0 |
| 37 | 0.1 | 0.4 |
| 38 | 0.25 | 1.2 |
| 39 | 0.1 | 1.0 |
| 40 | 25.0 | 35.0 |
| 41 | 0.3 | 3.5 |
| 42 | 0.1 | 0.7 |
| 43 | 0.08 | 0.7 |
| 44 | 1.2 | 2.0 |
| 51 | - | 0.1 |
| 52 | - | 0.1 |
| Total Pressure | $3.4 \times 10^{-7}$ torr | $5 \times 10^{-6}$ torr |

TABLE 4-3

Gases From the Loaded Pump With
Pressure x 10 Above Background

| AMU | Mixing Ratio in Source | Anticipated Jupiter Mixing Level | |
|---|---|---|---|
| 13 | $6 \times 10^{-6}$ | - | |
| 15 | $1 \times 10^{-4}$ | - | |
| 16 | $2 \times 10^{-4}$ | $7 \times 10^{-4}$ | ($CH_4$) |
| 17 | $1 \times 10^{-4}$ | $7 \times 10^{-6}$ to $2 \times 10^{-4}$ | ($NH_3$) |
| 29 | $2 \times 10^{-4}$ | - | |
| 34 | $2 \times 10^{-6}$ | $4 \times 10^{-7}$ | ($PH_3$) |
| 39 | $5 \times 10^{-6}$ | - | |
| 41 | $1 \times 10^{-5}$ | - | |

## 4.7 SUMMARY OF TEST RESULTS

The test results generally support the pumping model proposed in Section 2. Both hydrogen and helium are apparently pumped primarily by cathode burial. Hydrogen is pumped from five times to ten times faster than helium. A factor of three is accounted for by the ionization cross section difference, and is reflected in the discharge intensity. The rest of the difference is accounted for by the mass ratio, chemical activity differences and diffusion constants. Helium does not penetrate as deeply, combine chemically or diffuse farther in.

Some of the initially high hydrogen pumping can be explained by absorption from the vapor phase, causing marked time dependence for a few hundred seconds when admitting hydrogen to a fresh pump. Longer term decreases in pumping speeds of both hydrogen and helium are apparently associated with a loading of the cathodes within the volume that can be reached by the penetrating ions.

The argon model and pumping tests indicate an entirely different pumping mechanism for that gas, indicating that modifications which improve argon performance may have little effect on helium performance.

Even though the hydrogen pumping speed is high compared to nitrogen, the molecular conductance of the source is also 3.7 times higher, so the differential pumping factor is down. The large initial changes in hydrogen speeds are therefore reflected in the source pressure changes of 2-3% over the first few minutes of sample pumping.

The pump memory effects can be categorized as background gases which do not change with load, and evolved gases which increase with sample load. The background gases may be reduced by processing, but the evolved gases represent a serious source of error. Gases at 3 AMU and 17 AMU ($H_3^+$ and $NH_3^+$) were found to be created in the pump or mass spectrometer source at levels well above the anticipated mixing level in the Jovian atmosphere. Possibly excluding nitrogen from ever being pumped by the test pump would reduce the 17 AMU peak.

# 5. CONCLUSIONS AND RECOMMENDATIONS

The tests presented here demonstrate that the four liter per second flight sputter ion pump can be used to maintain the vacuum for the Jovian atmospheric entry mass spectrometer probe. It will pump the gas loads required for the mission without indication of instability or overloading. The special characteristics of hydrogen and helium, however, would not allow the pump to achieve a 100:1 differential pumping ratio which would be required to reduce the effects of the test pump on the source partial pressure to below 1 percent. The differential pumping ratio is affected by the high conductivity of the source for the light molecules as well as the limited speed of the pump for helium.

If the pumping of hydrogen and helium is stable, constant, or predictable even at a low speed, the instrument could still be calibrated for a 1 percent measurement. However, the hydrogen pumping speed showed short term changes sufficient to cause 3 percent source pressure error, and the helium pumping speed showed variations from one turn on to the next that would cause even greater errors. Additional attention to processing and cleaning the pump would very likely alleviate the helium pumping variability to a great extent. The short-term hydrogen changes, on the other hand, are apparently fundamental to the pumping processes that occur when the gas is admitted to a fresh pump. It is doubtful that either of these effects could be sufficiently predictable that the helium/hydrogen ratio could be measured to 1 percent after a long space flight.

Background, memory, and formation of species in the pump have serious consequences on the ability of the instrument to measure trace constituents on the Jovian mission. The large number of gases found in the pump would likely only be partially reduced by additional attention to processing.

One way to achieve many of the mission goals with a pump of this type is by utilizing a calibration gas sample in flight. By switching from a 90 percent hydrogen-10 percent helium calibration gas to the Jovian atmosphere, several advantages would be gained. First, the turn-on helium speed could be determined, and the pump could be run long enough to get past the initial large changes in hydrogen pumping speed. In addition, a baseline spectrum could be determined, and used to subtract the memory and background gases. The test results shown in Section 4 demonstrate that a gas load is necessary to obtain a meaningful baseline spectrum. The no load background is not sufficient.

Some of the higher level background and memory species would cause serious error in the trace measurements even with a calibrating gas baseline measurement. To limit these, careful attention must be paid to pump fabrication and processing. One of the most serious memory gases, from the standpoint of

mission goals, is at 17 amu, possibly ammonia. If this gas is ammonia, it could be reduced by limiting the pump's total exposure to nitrogen. High temperature bakeout of the pump parts and the pump after fabrication should reduce backgrounds, but the final bake of the fabricated instrument will be limited by the electron multiplier and the voltage feedthroughs. Choice of components which allow a higher temperature final bakeout will be important in the reduction of the background and memory effects.

In addition to the calibration gas and pump and instrument fabrication, some improvement could be made by modifications to the pump and to the source. First, the ion source should be designed with the lowest reasonable conductance. Assuming a factor can be gained there, we can turn to the pump design for changes which can further increase the differential pumping. The pump could be modified in its structure to achieve a higher discharge intensity, and it could be modified in materials of construction to achieve more efficient pumping of the ions, and to limit production of memory and background gases.

The geometry, as discussed in Section 2, could be changed to increase pumping speed in the $10^{-6}$ torr to $10^{-5}$ torr range at the sacrifice of pumping at lower pressures. This change would involve the use of more and smaller cells. Combinations of large and small cells could also be studied, to retain some pumping at the lowest pressures. These changes, together with correcting the mass scan problem mentioned in Section 4, could increase the helium speed to about 1.5 liters per second.

Attention to pump materials should be focused principally on the pumping of helium and on limiting the production of memory gases. Cathode materials which enable the helium to penetrate and diffuse should be studied, but such efforts might have only limited effect, since the present cathode materials allow deep penetration of the helium. Other materials which allow deeper penetration, such as carbon are unsuitable for other reasons.

One form that cathodes might take would be a thin metal coating on a glass or ceramic substrate. The metal would be required to maintain the potentials, but sufficiently thin so the helium atoms can penetrate into the glass where they can be buried or diffused.

Pump modifications directed at helium pumping speeds might deteriorate the speed of the pump for hydrogen and active gases. For this reason, a supplemental sublimation pump should be studied to retain the hydrogen performance. Proper design could also reduce or eliminate some of the pump memory by continually furnishing new surfaces and burying these undesired products. With a supplemental pump to handle hydrogen and active gases, the 100:1 differential pumping ratio could probably be achieved for all gases but helium. A workable design might feature a small ion pump for the helium at the center of a sublimation pump for the active gases.

In conclusion, even with each of the suggestions for pump modifications furnishing an improvement in the differential pumping ratio, the ratio will not approach the desired 100:1 figure with ion pumping alone. Therefore, future efforts should be directed primarily at reducing the memory and background gas, than at improving the differential pumping ratio. In-flight calibration gas runs will very likely be the only way to achieve a 1 percent precise measurement of the hydrogen to helium ratio. Since the pump specifications depend in this way on the overall instrument, and the way in which the experiment is performed, specific recommendations for future studies are not appropriate at the present time. When the mission is further defined by the Principal Investigator, the results presented here can be used as the basis for developing a practical pump for the mass spectrometer probe.

## REFERENCES


1. Kennedy, Atreya, and Carignan, NASA CR 137886 for Ames Research Center, Moffett Field, CA
2. Mary Rotheram, NASA CR 151944 for Ames Research Center, Moffett Field, CA
3. Jepsen, JAP 32, 2619 (1961)
4. Rutherford Proc. Am. Vac. Soc. Jan 1964
5. Rev. Mod. Phys. 38, 1, (1966)
6. KenKnight and Wehner, JAP 35, 322, 1964
7. Schiott, Can. Journ. Phys. 46, 449 (1968)
   Freeman and Lather, Can. Journ. Phys. 46, 467 (1968)
8. Jepsen Proc. of the Fourth Internl Vacuum Congress, 1968
9. Signmud, Can. Jour. Phys. 46, 731, (1968)
10. McDaniel, Collision Phenomena in Ionized Gases, John Wiley, N.Y., N.Y. 1964 p 19
11. Smith, JAP 38, 340 (1967)
12. Ion Scattering Spectrometer (ISS) 3M Co. Analytical Systems Div. Saint Paul, Minn
13. Anderson et al JAP 47, 13, (1976)
14. Ultek Technical Reprint D-1401
15. Carmichael, JAP 33, 1470 (1962)
16. Brubaker, 1959 Vac. Symp. Transactions
17. N. Ierokomos, NASA CR 111856 for NASA Langley Research Center (1971)
18. Rutherford, Vacuum 6, 2 (1966)
19. Dushman, Scientific Foundation of Vacuum Technique, John Wiley, N.Y. p 90 (1962)
20. Jepsen, Varian Technical Memo VR-7, Varian Associates, Palo Alto, CA
21. Dushman, (see Ref 19) p 170
22. Varian Ionization Gauge Instruction Sheet Model UNV-24